

Resonance phenomena in macroscopic quantum tunneling for an rf SQUID

Yu. N. Ovchinnikov*

L. D. Landau Institute for Theoretical Physics, Academy of Sciences of Russia, Kossigin Str. 2, 119334 Moscow, Russia

P. Silvestrini, V. Corato, and S. Rombetto

Dipartimento di Ingegneria dell'Informazione, Seconda Università di Napoli, I-81031 Aversa, Italy

(Received 10 May 2004; revised manuscript received 23 September 2004; published 28 January 2005)

We consider the theoretical problem of resonant phenomena in the macroscopic quantum tunneling for an rf superconducting quantum interference device in the presence of an external irradiating field. The transition probability between different flux states is studied by varying the external parameters of the double-well potential describing the system in a way that the pumping level in the left potential well is close to one of the levels in the right potential well. The dependence of the transition probability on the external drive of the system shows two resonance peaks, the former connected with the *resonant tunneling* and the latter with the *resonant pumping*. The relative position of the peaks depends on the pumping frequency ω and on the system parameters.

DOI: 10.1103/PhysRevB.71.024529

PACS number(s): 74.50.+r, 03.65.Yz, 03.67.Lx

I. INTRODUCTION

A Josephson device is a macroscopic quantum object, and the possibility to observe coherent and incoherent macroscopic quantum phenomena has attracted great interest both from the theoretical¹ and experimental² sides. The first phenomena investigated are the decay from metastable states by macroscopic quantum tunneling³ (MQT) and energy level quantization^{4,5} (ELQ). Furthermore, in recent experiments,⁶ evidence of the superposition between macroscopically distinct quantum states (MQC) in both single Josephson junctions and superconducting-quantum-interference-device (SQUID-) based systems under the action of an external microwave has been observed. In fact the possibility to control the quantum dynamics of Josephson systems by microwave irradiation is a very powerful technique also in view of the application of these devices to quantum computation.⁷ In this paper we present a theoretical approach to describe the quantum behavior of a macroscopic system interacting with an external field at frequencies close to resonant conditions. Moreover, we apply our results to simulate resonant phenomena in rf SQUID's, whose parameters lie in the range typically used in the experiments.⁸

As first pointed out by Caldeira and Leggett,¹ in order to observe quantum effects in a macroscopic system, the quantum system must be essentially decoupled from the degrees of freedom describing the environment. The interaction with the external thermal bath produces the appearance of the finite width γ of quantum levels,⁹ leading to relaxation and decoherence effects.

In the problem of quantum tunneling it is possible to distinguish three regions, differing for the value of the damping parameter γ which is equal to the one-half of the sum of the transition probabilities between the energy states.¹⁰ In the first region, corresponding to the overdamped regime, γ is larger than the plasma frequency ω_J —that is, the distance between levels close to the bottom of the potential well. The second regime is the moderate underdamped one, as γ is much smaller than the plasma frequency, but larger than the

probability of quantum tunneling under the potential barrier. In this region, the quantum tunneling probability is depressed by dissipation.¹¹ The third region corresponds to the extremely underdamped limit, as γ is much smaller than the probability of quantum tunneling. This condition is hard to achieve and can be better realized for levels close to the barrier top in the double-well potential.

Resonant phenomena can take place only if the energy width γ is small compared to the energy difference between levels, $\gamma \ll \omega_j$.

Transitions between levels can occur either by thermal activation inside the same potential well or by tunneling between resonant levels in different wells (see Fig. 1). Interesting aspects for experiments on Josephson devices are realized when the states involved in the transition correspond to macroscopically distinct ones, such as, for instance, different flux states in a rf-SQUID. In this case the interacting energy states can be visualized as belonging to different wells of the double-well potential sketched in Fig. 1 and the transition process is characterized by tunneling across the potential barrier. The nonzero width of levels leads to a reduction of coherence during the tunneling process¹¹ and in such a case

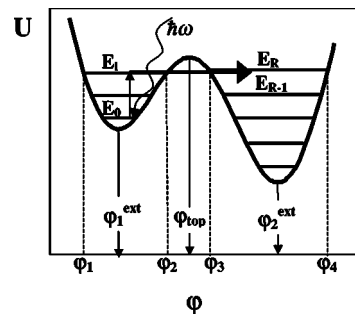


FIG. 1. A sketch of an rf-SQUID double-well potential $U(\varphi)$, with two minima located at φ_1^{ext} and φ_2^{ext} . φ_{top} is the position of the potential maximum. The turning points for the two energy levels E_L and E_R are φ_1, φ_2 and φ_3, φ_4 , respectively.

the behavior of the system strictly depends on the ratio between the two small parameters γ and T_N , where T_N is the tunneling amplitude.¹¹

In the following we consider the resonant tunneling assisted by microwave irradiation under the condition $\gamma \gg T_N$, as occurs in dissipative systems, in the moderate underdamped quantum regime. As shown in Fig. 1, the process can be visualized as a resonant pumping from the ground state to the upper excited level, followed by resonant tunneling from the left well to the right one (photon-activated resonant tunneling). The condition $\gamma \gg T_N$ requires that the excited level in resonance with the microwave should not be too close to the top of the potential barrier. Otherwise the tunneling process may become the dominant transition with respect to the thermally induced decay between levels in the same well. Due to the very strong exponential dependence of the tunneling amplitude on the energy of levels, the macroscopic tunneling can really be observed only if the number of levels in the left potential well is not large (say less than 10).¹⁰

II. TUNNELING TRANSITION PROBABILITY W FROM THE LEFT POTENTIAL WELL TO THE RIGHT ONE IN RESONANT CONDITIONS

In describing the photon-activated resonant tunneling, great relevance must be given to the excited level in the left well, hereafter referred to as the *pumped level*, whose population is increased by the external irradiation, and the two nearest levels in the right well. The tunneling transition probability decreases very quickly for states below the barrier top, such as $e^{-2\pi n}$, where n is the number of states counted from the barrier top.¹² As a consequence we can neglect transitions into lower levels in the right potential well.

To calculate the distribution function for the quantum tunneling in the resonant pumping case, we can start from the rf-SQUID Hamiltonian of zero approximation in the presence of an external field with frequency ω and intensity \mathfrak{J} , which can be written as

$$H = -\frac{1}{2M} \frac{\partial^2}{\partial \varphi^2} + U_0 \left\{ \frac{1}{2} (\varphi - \varphi_x)^2 + \beta_L \cos \varphi \right\} + \frac{\mathfrak{J}}{2e} \cos(\omega t) \varphi, \quad (1)$$

where the mass M is connected to the junction capacitance C and the β_L SQUID parameter depends on the superconducting loop inductance L and the Josephson current I_c :

$$M = \left(\frac{\hbar}{2e} \right)^2 C, \quad \beta_L = \frac{2\pi L I_c}{\Phi_0}. \quad (2)$$

$U_0 = (\Phi_0/2\pi)^2 (1/L)$ is the relevant energy scale and Φ_0 is the flux quantum. The external magnetic flux φ_x is a free parameter of the system. By varying the parameters U_0 and φ_x we can control the relative position of levels in the left and right potential wells with respect to the pumping frequency. It is worth noting that the last term in the Eq. (1) is the high-frequency external pumping.

The interaction with the “environment” is described by the effective action $A(\varphi, \bar{\varphi})$, as reported in Ref. 10. For sharp levels $\gamma \ll \omega_j$, we can write down the rate equation for the

density matrix elements ρ_ℓ^j in the form of a differential equation.⁹

$$\begin{aligned} \frac{\partial \rho_\ell^j}{\partial t} = & \frac{i\mathfrak{J}}{2e} \cos \omega t \sum_m \{ \langle j|\varphi|m\rangle \exp[-i(E_m - E_j)t] \rho_\ell^m \\ & - \langle m|\varphi|\ell\rangle \exp[i(E_m - E_\ell)t] \rho_m^j \} + \sum_{m,n} W_{\ell n}^{jm} \rho_n^m \\ & - \frac{1}{2} \sum_m (W_{mj}^{mj} + W_{m\ell}^{m\ell}) \rho_\ell^j. \end{aligned} \quad (3)$$

For the density matrix, we work in the basis of the states of the system, decoupled from the environment.^{9,10}

Assuming that the Josephson junction is shunted by the normal resistance R ,⁵ in the low-temperature region all transition elements related to R are given by the expression⁹

$$\begin{aligned} W_{\ell n}^{jm} = & \frac{\pi}{2e^2 R} \left(1 + th \frac{\tilde{\omega}}{2T} \right) M(\tilde{\omega}) \left[\langle j|\exp\left(i\frac{\varphi}{2}\right)|m\rangle \langle \ell| \right. \\ & \times \exp\left(-i\frac{\varphi}{2}\right)|n\rangle + \langle j|\exp\left(-i\frac{\varphi}{2}\right)|m\rangle \langle \ell|\exp\left(i\frac{\varphi}{2}\right)|n\rangle \left. \right], \end{aligned} \quad (4)$$

where

$$\tilde{\omega} = \frac{E_m - E_j + E_n - E_\ell}{2}, \quad (5)$$

$$M(\tilde{\omega}) = \frac{\tilde{\omega}}{\pi} \coth \frac{\tilde{\omega}}{2T} \rightarrow \frac{|\tilde{\omega}|}{\pi}. \quad (6)$$

At low temperatures and for weak pumping power, only two nondiagonal matrix elements are different from zero: ρ_ℓ^0 and ρ_0^ℓ . Hence we obtain from Eq. (3)

$$\frac{\partial \rho_\ell^0}{\partial t} = -\frac{i\mathfrak{J}}{2e} \cos \omega t \langle 0|\varphi|\ell\rangle \exp(i(E_0 - E_\ell)t) - \frac{1}{2} \sum_{m < \ell} W_{m\ell}^{m\ell} \rho_\ell^0. \quad (7)$$

Then the solution of Eq. (7) is

$$\rho_\ell^0 = -\frac{\mathfrak{J}}{4e} \langle 0|\varphi|\ell\rangle \frac{\exp\{i[\omega - (E_\ell - E_0)]t\}}{\omega - (E_\ell - E_0) - i\gamma_\ell}, \quad \rho_0^\ell = (\rho_\ell^0)^* \quad (8)$$

with

$$\gamma_\ell = \frac{1}{2} \sum_{m < \ell} W_{m\ell}^{m\ell}. \quad (9)$$

Equation (7) indicates that only one level ℓ is close to the resonance. Note that the transition matrix element $\langle 0|\varphi|\ell\rangle$ depends strongly on the energy of the state ℓ .^{12,13} For the same reason it is enough to take in sum over m in Eq. (9) only one term with $m = \ell - 1$; hence,

$$\gamma_\ell = \frac{E_\ell - E_{\ell-1}}{\text{Re}^2} \left| \langle \ell - 1 | \exp\left(i\frac{\varphi}{2}\right) | \ell \rangle \right|^2. \quad (10)$$

The function ρ_ℓ^ℓ satisfies the following equation coming from Eqs. (3) and (8) for the matrix element ρ_ℓ^0 :

$$\frac{\partial \rho_\ell^\ell}{\partial t} = \frac{i\mathcal{I}^2}{16e^2} |\langle \ell | \varphi | 0 \rangle|^2 \left(\frac{1}{\omega - (E_\ell - E_0) + i\gamma_\ell} - \frac{1}{\omega - (E_\ell - E_0) - i\gamma_\ell} \right) - 2\gamma_\ell \rho_\ell^\ell. \quad (11)$$

Then the solution of Eq. (11) is

$$\rho_\ell^\ell = \frac{\mathcal{I}^2}{16e^2} \left(\frac{|\langle \ell | \varphi | 0 \rangle|^2}{[\omega - (E_\ell - E_0)]^2 + \gamma_\ell^2} \right). \quad (12)$$

According to Ref. 11, the transition probability W from the left potential well to the right one is given by the equation

$$W = 2|T_\ell|^2 \rho_\ell^\ell \exp(-2\alpha C_{\text{Eu}}) \Gamma(1-2\alpha) \times \left(\frac{(E_\ell - E_R)^2 + (\gamma_\ell + \gamma_R)^2}{\omega_j^2} \right)^\alpha \frac{1}{\sqrt{(E_\ell - E_R)^2 + (\gamma_\ell + \gamma_R)^2}} \times \cos \left[\pi\alpha - (1-2\alpha) \arctan \left(\frac{E_\ell - E_R}{\gamma_\ell + \gamma_R} \right) \right]. \quad (13)$$

In Eq. (13) the quantity C_{Eu} is the Euler constant, T_ℓ the tunneling amplitude from the energy level E_ℓ , and α a dimensionless constant. (E_ℓ, γ_ℓ) and (E_R, γ_R) are the level positions and the widths of levels in the left and right wells, respectively. The quantities α , T_ℓ , and γ_R will be numerically estimated in the following.

In Fig. 4 below, we give the transition probability W as function of φ_x for three values of irradiation frequency ω . The position of the first peak, connected to the resonant tunneling from the upper state in the left potential well to the right potential well, takes place at a fixed value of $\varphi_x^{(0)}$ (left peak in Fig. 4). The position of the second peak, connected to the resonant pumping to the upper excited state, moves to the right as the pumping frequency is increased.

III. CALCULATION OF THE LEVEL POSITION AND TRANSITION MATRIX ELEMENTS

In order to proceed in the calculation of W , we first introduce the quantity γ , the width of the first level. Defining φ_1^{ext} and φ_2^{ext} as the positions of the two minima of the potential U (see Fig. 1), near the minima we have

$$U(\varphi) = U(\varphi_{1,2}^{\text{ext}}) + U_{1,2}^{\text{ext}}(\varphi - \varphi_{1,2}^{\text{ext}})^2, \quad (14)$$

where

$$U_{1,2}^{\text{ext}} = \frac{U_0}{2} [1 - \beta_L \cos(\varphi_{1,2}^{\text{ext}})]. \quad (15)$$

The wave function of the first excited state can be taken in the parabolic potential approximation:

$$\Psi_1 = \frac{(8MU_1^{\text{ext}})^{1/8}}{(2\pi)^{1/4}} \mathcal{D}_1[(8MU_1^{\text{ext}})^{1/4}(\varphi - \varphi_1^{\text{ext}})], \quad (16)$$

where \mathcal{D}_1 is the parabolic cylinder function.¹⁴ The wave function Ψ_0 of the ground state can be written as

$$\Psi_0 = \frac{(8MU_1^{\text{ext}})^{1/8}}{(2\pi)^{1/4}} \exp\left(-\int_{\varphi_1^{\text{ext}}}^{\varphi} d\varphi \sqrt{2M[U(\varphi) - U(\varphi_1^{\text{ext}})]}\right). \quad (17)$$

This form will be used for calculation of the transition matrix element $\langle 0 | \varphi | \ell \rangle$. From Eqs. (10), (16), and (17), we find the quantity γ .

$$\gamma = \frac{1}{8M \text{Re}^2}. \quad (18)$$

The quantity α is connected to γ (Ref. 11):

$$\alpha = \frac{\gamma}{\pi} M(\varphi_2^{\text{ext}} - \varphi_1^{\text{ext}})^2 = \frac{(\varphi_2^{\text{ext}} - \varphi_1^{\text{ext}})^2 \hbar}{8\pi \text{Re}^2}. \quad (19)$$

We suppose the energies E_ℓ and E_R be close to the barrier top (Fig. 1), so that the transition matrix element $|T_\ell|^2$ is given by the expression

$$|T_\ell|^2 = \frac{\Omega_\ell \Omega_R}{4\pi^2} \exp\left(-\pi\sqrt{2MU_1} \frac{U_{\text{top}} - E_\ell}{U_1}\right), \quad (20)$$

where

$$U_1 = -\frac{U_0}{2}(1 - \beta_L \cos \varphi_{\text{top}}) \quad (21)$$

and Ω_ℓ and Ω_R are the distances between neighbor levels in left and right potential wells:

$$\Omega_\ell = E_\ell - E_{\ell-1}, \quad \Omega_R = E_R - E_{R-1}. \quad (22)$$

The position of levels can be found with the help of the quasiclassical approximation⁹

$$\begin{aligned} \cos\left(\Phi_1 + \frac{\chi}{2}\right) &= 0, \quad \text{for levels in the left potential well,} \\ \cos\left(\Phi_2 + \frac{\chi}{2}\right) &= 0, \quad \text{for levels in the right potential well.} \end{aligned} \quad (23)$$

The phases $\Phi_{1,2}$ and χ are defined by the following equations:

$$\begin{aligned} \Phi_1 &= \int_{\tilde{\varphi}_1}^{\varphi_{\text{top}}} d\varphi \sqrt{2M[U_{\text{top}} - U(\varphi)]} \\ &+ \frac{M(U_{\text{top}} - E)}{\sqrt{2MU_1}} \ln\left(\frac{2^{1/4}}{8(MU_1)^{1/4}(\varphi_{\text{top}} - \tilde{\varphi}_1)}\right) \\ &- M(U_{\text{top}} - E) \int_{\tilde{\varphi}_1}^{\varphi_{\text{top}}} d\varphi \left(\frac{1}{\sqrt{2M[U_{\text{top}} - U(\varphi)]}} \right. \\ &\left. - \frac{\sqrt{\varphi_{\text{top}} - \tilde{\varphi}_1}}{\sqrt{2MU_1(\varphi_{\text{top}} - \varphi)^2(\varphi - \tilde{\varphi}_1)}} \right), \end{aligned}$$

$$\begin{aligned} \Phi_2 = & \int_{\varphi_{top}}^{\tilde{\varphi}_4} d\varphi \sqrt{2M[U_{top} - U(\varphi)]} \\ & + \frac{M(U_{top} - E)}{\sqrt{2MU_1}} \ln \left(\frac{2^{1/4}}{8(MU_1)^{1/4}(\tilde{\varphi}_4 - \varphi_{top})} \right) \\ & - M(U_{top} - E) \int_{\varphi_{top}}^{\tilde{\varphi}_4} d\varphi \left(\frac{1}{\sqrt{2M[U_{top} - U(\varphi)]}} \right. \\ & \left. - \frac{\sqrt{\tilde{\varphi}_4 - \varphi_{top}}}{\sqrt{2MU_1}(\varphi_{top} - \varphi)^2(\tilde{\varphi}_4 - \varphi)} \right), \\ \Gamma \left(\frac{1 + i\lambda}{2} \right) = & \frac{\sqrt{2\pi} \exp(-\pi\lambda/4)}{\sqrt{1 + \exp(-\pi\lambda)}} \exp(i\chi), \\ U(\tilde{\varphi}_1) = & U(\tilde{\varphi}_4) = U(\varphi_{top}), \\ \lambda = & \sqrt{2MU_1} \frac{U_{top} - E}{U_1}. \end{aligned} \quad (24)$$

$$\lambda = \sqrt{2MU_1} \frac{U_{top} - E}{U_1}. \quad (25)$$

Note that, in the limiting cases, the phase χ is given by

$$\begin{aligned} \chi = & (\lambda/2)\psi(1/2) \\ \text{for } \lambda \ll 1 \text{ with } \psi(1/2) = & -C_{Eu} - 2 \ln 2 = -1.96351, \\ \chi = & (\lambda/2) \ln[(\lambda/2) - 1] \quad \text{for } \lambda \gg 1. \end{aligned} \quad (26)$$

Furthermore, for the arbitrary value of λ , we have

$$\chi = \lambda/2 \psi(1/2) - \sum_{k=0}^{\infty} \left(\arctan \frac{\lambda}{2k+1} - \frac{\lambda}{2k+1} \right). \quad (27)$$

Now to complete our considerations, we can give the expressions for the wave functions ψ_ℓ , $\psi_{\ell-1}$, ψ_R , and ψ_{R-1} . In the quasiclassical approximation, we have

$$\begin{aligned} \psi_\ell = & \frac{1}{G_\ell} \frac{1}{[2M(E - U)]^{1/4}} \sin \left(\frac{\pi}{4} + \int_{\varphi_1}^{\varphi} d\varphi \sqrt{2M[E_\ell - U(\varphi)]} \right), \\ \ell \rightarrow & \ell, \ell - 1, \\ \psi_R = & \frac{1}{G_R} \frac{1}{[2M(E - U)]^{1/4}} \sin \left(\frac{\pi}{4} + \int_{\varphi}^{\varphi_4} d\varphi \sqrt{2M[E_R - U(\varphi)]} \right), \\ R \rightarrow & R, R - 1, \end{aligned} \quad (28)$$

where $G_{l,R}$ are the normalized factors:

$$\begin{aligned} G_\ell^2 = & \frac{1}{2} \int_{\varphi_1}^{\varphi_2} \frac{d\varphi}{\sqrt{2M[E_\ell - U(\varphi)]}}, \quad E_\ell = U(\varphi_{1,2}), \\ G_R = & \frac{1}{2} \int_{\varphi_3}^{\varphi_4} \frac{d\varphi}{\sqrt{2M[E_R - U(\varphi)]}}, \quad E_R = U(\varphi_{3,4}). \end{aligned} \quad (29)$$

The energy levels E_ℓ and E_R are solutions of Eqs. (23) and (24). The label ℓ (R) notes the states in the left (right) potential well.

The width of the levels γ_ℓ and γ_R can be found with the help of Eqs. (10) and (28). The transition matrix element

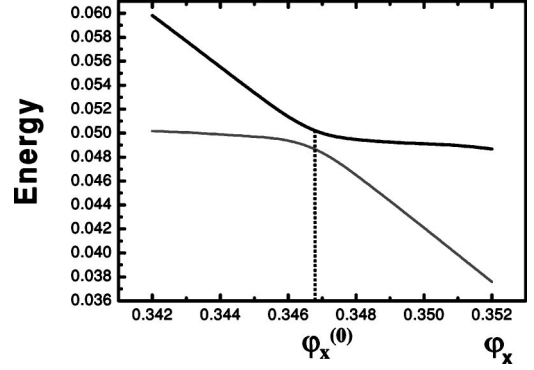


FIG. 2. The anticrossing diagram of levels E_ℓ and E_R as a function of the external flux φ_x . In the absence of the repulsion term due to λ , the “crossing” of levels E_ℓ and E_R would occur at some point, addressed as $\varphi_x^{(0)}$. The exact level positions are obtained as solutions of Eq. (31) by varying φ_x . Energies are referred to the bottom of the left potential well and are computed with the following parameters: $\beta_L=1.75$, $L=210$ pH, and $C=0.1$ pF, leading to $\sqrt{MU_0}=22.412$.

$\langle 0|\varphi|\ell\rangle$, which is involved in Eqs. (12) and (13) can be found with the help of Eqs. (17) and (28), as

$$\begin{aligned} \langle 0|\varphi|\ell\rangle = & \frac{(8MU_1^{ext})^{1/8}}{(2\pi)^{1/4}G_\ell} \int_{\varphi_1}^{\varphi_2} \frac{d\varphi(\varphi - \varphi_1^{ext})}{\{2M[E_\ell - U(\varphi)]\}^{1/4}} \\ & \times \exp \left(- \int_{\varphi_1^{ext}}^{\varphi} d\varphi \sqrt{2M[U(\varphi) - U(\varphi_1^{ext})]} \right) \\ & \times \sin \left(\frac{\pi}{4} + \int_{\varphi_1}^{\varphi} d\varphi \sqrt{2M[E_\ell - U(\varphi)]} \right). \end{aligned} \quad (30)$$

IV. TRANSITION MATRIX ELEMENTS BETWEEN STATES CLOSE TO THE BARRIER TOP

We suppose that the initial value of the external parameters U_0 and φ_x is such that there are two close levels E_ℓ and E_R near the top of the barrier (but not too close, $\lambda \geq 1$). We consider that the change of the external parameter φ_x (or both U_0 and φ_x) leads to the “crossing” of levels E_ℓ and E_R in some point $\varphi_x^{(0)}$ (Fig. 2). Furthermore, when the high-frequency field ω crosses the energy difference between ground and the upper levels in the left well, $\Delta E_\ell = E_\ell - E_0$, another point $\varphi_x^{(1)}$ is defined (Fig. 3). The transition probability W will have two sharp peaks in these two points (Fig. 4).

Curves presented in Figs. 2–7 are obtained by assuming the following parameters: $\beta_L=1.75$, $L=210$ pH, and $C=0.1$ pF, leading to $\sqrt{MU_0}=22.412$ and $R=6$ k Ω .

Since levels E_ℓ and E_R are placed near the barrier top φ_{top} , the width of levels and especially the transition matrix element $\langle 0|\varphi|\ell\rangle$ (if $\ell \neq 1$) are very sensitive to the value of energy E_ℓ and hence to the value of the external parameter φ_x . Strictly speaking in such a situation the dependence of E_ℓ (or E_R) on the parameter φ_x is nonlinear. The exact equation for the position of levels near the barrier top in the case of small viscosity can be cast in the form

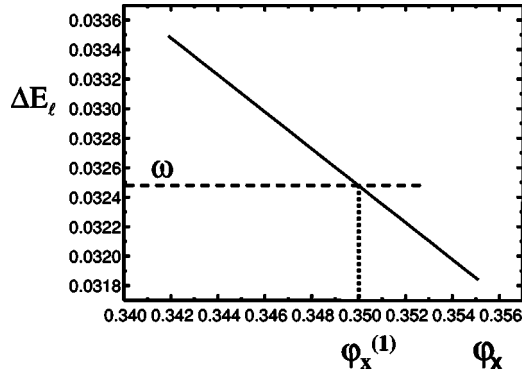


FIG. 3. The crossing between the high-frequency pumping field ω and the energy difference between the ground and upper levels in the left well, $\Delta E_\ell = E_\ell - E_0$, defines the point $\varphi_x^{(1)}$.

$$\cos(\Phi_1 - \Phi_2) + \cos(\Phi_1 + \Phi_2 + \chi)[1 + \exp(-\pi\lambda)]^{1/2} = 0. \quad (31)$$

Equation (31) describes the repulsion of levels E_ℓ and E_R giving the “anticrossing” picture. In fact the exact level positions as a function of the external “drive” of the potential, φ_x , is shown in Fig. 2. In Fig. 4 we present the behavior of W as a function of φ_x . The first peak, associated with the tunneling phenomenon, appears for a fixed external flux. The second peak, due to the pumping process, moves with the irradiation field frequency [Figs. 4(a) and 4(b)] until it superimposes onto the first peak [Fig. 4(c)].

Furthermore, with high accuracy, the transition matrix elements can be found with the help of quasiclassical approximation¹⁵ even for transitions in the ground state.¹⁰ The transition matrix element between states (p, j) can be taken in the form

$$\langle p | \xi | j \rangle = \frac{\omega(E)}{(2\pi)} \oint dt \xi(t) \exp[-i\omega(E)(p-j)t], \quad (32)$$

where $\omega(E)$ is the classical frequency of motion for the energy $E = (E_j + E_p)/2$. This energy is counted from the bottom of the potential well. Using the cubic approximation for the potential well,

$$U(\varphi) = U_1^{ext}(\varphi - \varphi_1^{ext})^2 \left[1 - \frac{2(\varphi - \varphi_1^{ext})}{3(\varphi_{top} - \varphi_1^{ext})} \right]. \quad (33)$$

The classical equation of motion is

$$M \frac{\partial^2 Z}{\partial t^2} = -2U_1^{ext} Z \left(1 - \frac{Z}{\varphi_{top} - \varphi_1^{ext}} \right) \quad \text{where } Z = \varphi - \varphi_1^{ext}. \quad (34)$$

The solution of Eq. (34) is given by the Jacobian elliptic function sn:

$$Z = Z_1 + (Z_2 - Z_1) \text{sn}^2 \left(t \sqrt{\frac{U_1^{ext}(Z_3 - Z_1)}{3M(\varphi_{top} - \varphi_1^{ext})}} \right), \quad (35)$$

where Z_1, Z_2, Z_3 are solutions of the equation $E = U$ and are given by the relations

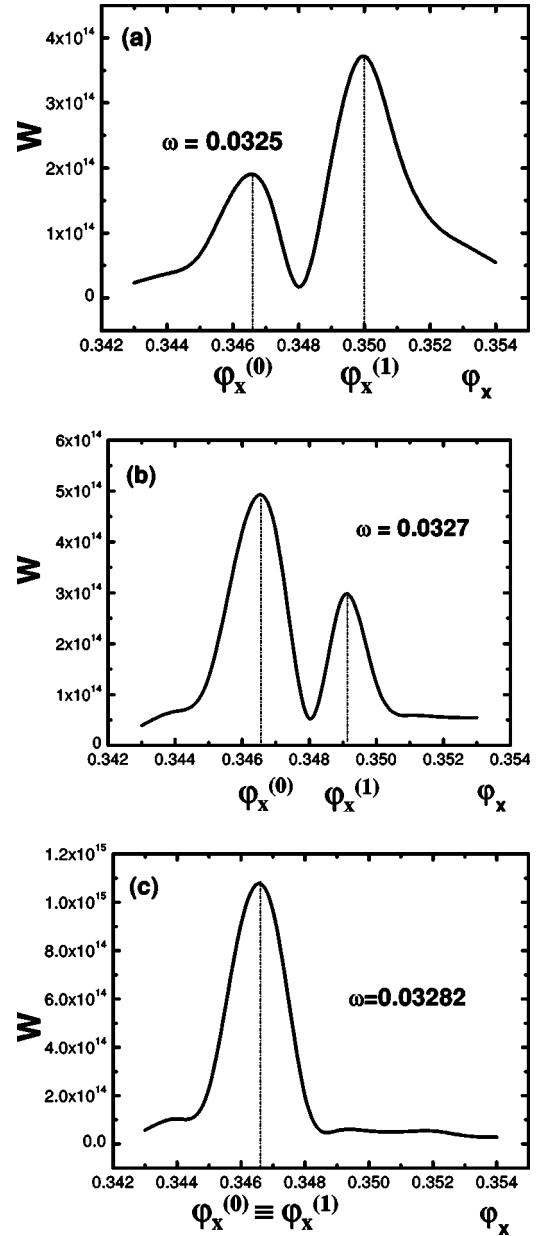


FIG. 4. Transition probability W as function of φ_x . The curve is calculated according to Eq. (13) for different values of the pumping frequency. The two peaks shown in (a) and (b) are connected to effects of the resonant tunneling between levels in different wells and the resonant pumping between levels in the same well. As predicted, the peak due to the resonant pumping moves with the pumping frequency until it superimposes to the tunneling peak, as evident in (c). Curves are obtained by using the following parameters: $\beta_L = 1.75$, $L = 210$ pH, $C = 0.1$ pF, and $R = 6$ k Ω . W is normalized to the term $\mathcal{I}^2/16e^2$.

$$Z_1 = (\varphi_{top} - \varphi_1^{ext}) \left[\frac{1}{2} + \sin \left(-\frac{\pi}{3} + \frac{\alpha}{3} \right) \right],$$

$$Z_2 = (\varphi_{top} - \varphi_1^{ext}) \left[\frac{1}{2} - \sin \left(\frac{\alpha}{3} \right) \right],$$

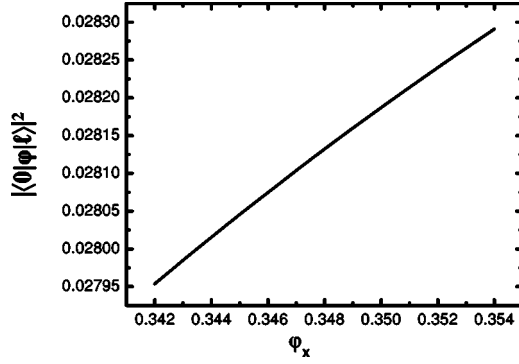


FIG. 5. Squared transition matrix element $|\langle 0|\varphi|\ell\rangle|^2$ as a function of φ_x as numerically calculated according to Eq. (39) with $\beta_L=1.75$, $L=210$ pH, and $C=0.1$ pF.

$$Z_3 = (\varphi_{top} - \varphi_1^{ext}) \left[\frac{1}{2} + \sin\left(\frac{\alpha}{3}\right) \right],$$

$$\alpha = \arcsin\left(1 - \frac{6E}{U_1^{ext}(\varphi_{top} - \varphi_1^{ext})}\right). \quad (36)$$

The function $\text{sn}^2(u)$ is defined as

$$\text{sn}^2(u) = \frac{1}{k^2} \left(1 - \frac{E(k)}{K(k)}\right) - \left(\frac{\pi}{kK}\right)^2 \sum_{L \neq 0} \frac{Lq^L}{1 - q^{2L}} \exp\left(\frac{i\pi Lu}{K}\right), \quad (37)$$

with $k = \sqrt{(Z_2 - Z_1)/(Z_3 - Z_1)}$, $K = K(k)$, $E(k)$ the complete elliptic integrals, $q = \exp(-\pi K'/K)$, $K' = K(k')$, and $k' = \sqrt{1 - k^2}$.

The energy of the ground state, E_0 , can be estimated as

$$E_0 = \frac{1}{2} \sqrt{\frac{2U_1^{ext}}{M} \left[1 - \frac{5}{24\sqrt{2MU_1^{ext}(\varphi_{top} - \varphi_1^{ext})}}\right]}. \quad (38)$$

The transition matrix element [Eq. (32)] with help of Eq. (37) can be cast in the form

$$\langle p|\varphi|j\rangle = -\frac{Z_2 - Z_1}{2} \left(\frac{\pi}{kK}\right)^2 \frac{(j-p)}{\sinh\left(\frac{\pi(j-p)K'}{K}\right)}. \quad (39)$$

If many levels are in the right potential well, the cubic approximation may be not adequate, and in general we have

$$\langle p|\xi|j\rangle = \frac{2}{T} \int_0^{T/2} dt \xi(t) \cos[\omega(E)(j-p)t],$$

$$\left(\frac{\partial\varphi}{\partial t}\right)^2 = \frac{2(E-U)}{M}. \quad (40)$$

In Eq. (40) the quantity T is the period of classical motion, $T=2\pi/\omega(E)$. In the initial motion ($t=0$), the ‘‘particle’’ is placed in the left ‘‘turning’’ point. We can numerically calculate the transition matrix element $\langle 0|\varphi|\ell\rangle$ by both Eqs. (30) and (39). Although we get a very good agreement with these two different calculations, we show in Fig. 5 the results

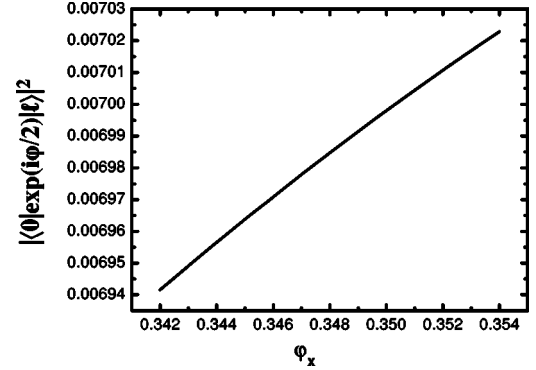


FIG. 6. Squared transition matrix element $|\langle 0|\exp(i\varphi/2)|\ell\rangle|^2$ as a function of φ_x as numerically calculated according to Eq. (40) with $\beta_L=1.75$, $L=210$ pH, and $C=0.1$ pF.

coming from Eq. (39). The width γ_R can be taken in the following form [see Eq. (10)]:

$$\gamma_R = \frac{\omega(E)}{\text{Re}^2} \left| \langle R-1|\exp\left(\frac{i\varphi}{2}\right)|R\rangle \right|^2,$$

$$E = \frac{E_R + E_{R-1}}{2}. \quad (41)$$

Finally, the results of numerical calculations of the squared transition matrix elements $|\langle 0|\exp(i\varphi/2)|\ell\rangle|^2$ and $|\langle R-1|\exp(i\varphi/2)|R\rangle|^2$ are given in Figs. 6 and 7, respectively.

Transition matrix elements are essential for the resonant tunneling, as they appear to be not constant even in the resonance region. The dependence of the transition matrix elements on φ_x leads to a shift of the peaks, as well as to a more complex shape than a simple Lorentzian one. Both effects are observed in Fig. 4. For this reason we present a numerical calculation of the transition matrix elements in Figs. 5–7.

V. CONCLUSION

In conclusion we have developed a theoretical approach to study resonant phenomena in macroscopic quantum tun-

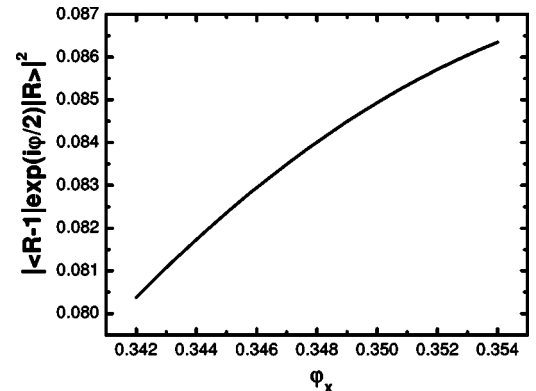


FIG. 7. Squared transition matrix element $|\langle R-1|\exp(i\varphi/2)|R\rangle|^2$ as a function of φ_x as numerically calculated according to Eq. (40) with $\beta_L=1.75$, $L=210$ pH, and $C=0.1$ pF.

neling in the presence of an external irradiating field, limiting ourselves to the moderate underdamped quantum regime $\gamma \gg T_N$. The transition probability W from the left potential well to the right one, as well as the anticrossing diagram of levels and the transition matrix elements in the left and in the right potential well, is numerically calculated for a rf-SQUID as functions of the external flux φ_x . We focused our attention on the effect of resonant pumping on the transition probability in a condition for which the excited *pumped level* in the left potential well is close to a level in the right potential well. The dependence of the transition probability W on the external parameter φ_x (see Fig. 4) shows two peaks. The first is connected with the *resonant tunneling* and the second one is associated with the *resonant pumping*. The relative positions of these two peaks strictly depend on the pumping frequency and on the external flux biasing the SQUID.

The transition probability W from the left potential well to the right one is obtained as a function of the potential parameters and of the shunt resistance R . Assuming that the temperature T of the thermal bath is negligible in comparison with the plasma frequency—the distance between levels in left (right) potential well—Eq. (13) for W can be easily generalized for the case of moderate high temperatures, as T is orders of magnitude smaller than the distance between levels or the width of levels $\gamma_{\ell,R}$ (see Ref. 11). The predicted phenomena have been observed by escape measurements.⁶

Work is in progress to extend such a theoretical treatment to the case of the small-viscosity limit $\gamma \approx T_N$ which in experiments means to consider the extremely underdamped case for an rf-SQUID under the action of external microwaves.

Note that, in the considered problem, the existence of other levels except the two resonant levels ($E_{\ell,R}$) in left (right) potential well is essential. The transition to levels with energy E smaller than ($E_{\ell,R}$) determinates the width of these levels and the transition probability W from the left to the right potential well. The idealized model, where such states are not taken into account, can be valid only in the small-time interval $t < (\gamma_{\ell} + \gamma_R)^{-1}$ (see Ref. 16).

ACKNOWLEDGMENTS

We are grateful to Berardo Ruggiero for the interesting scientific discussions and hints. The research of one of us (Yu.N.O.) is supported by Cariplo Foundation-Italy, CRDF-USA under Grant No. RPI-2565-MO-03 and the Russian Foundation of Basic Research. This work has been partially supported by MIUR-FIRB under Project “Nanocircuiti a Superconduttore” and by MIUR-COFIN under Project “Josephson Networks for Quantum Coherence and Information.”

*Electronic address: ovc@itp.ac.ru

¹A. O. Caldeira and A. J. Leggett, Phys. Rev. Lett. **46**, 211 (1981); D. V. Averin, J. R. Friedman, and J. E. Lukens, Phys. Rev. B **62**, 11 802 (2000).

²*Quantum Computing and Quantum Bits in Mesoscopic Systems*, edited by A. J. Leggett, B. Ruggiero, and P. Silvestrini (Kluwer Academic, Dordrecht, 2004).

³D. B. Schwartz, B. Sen, C. N. Archie, and J. E. Lukens, Phys. Rev. Lett. **55**, 1547 (1985); S. Washburn, R. A. Webb, R. F. Voss, and S. M. Faris, *ibid.* **54**, 2712 (1985); V. Corato, S. Rombetto, P. Silvestrini, C. Granata, R. Russo, and B. Ruggiero, Supercond. Sci. Technol. **17**, S385 (2004).

⁴J. M. Martinis, M. H. Devoret, and J. Clarke, Phys. Rev. Lett. **55**, 1543 (1985); Phys. Rev. B **35**, 4682 (1987).

⁵P. Silvestrini, V. G. Palmieri, B. Ruggiero, and M. Russo, Phys. Rev. Lett. **79**, 3046 (1997).

⁶J. R. Friedman, V. Patel, W. Chen, S. K. Tolpygo, and J. E. Lukens, Nature (London) **406**, 43 (2000); C. H. van der Wal, A. C. J. Ter Haar, F. K. Wilhem, R. N. Schouten, J. P. M. Harmaas, T. P. Orlando, S. Lloyd, and J. E. Mooij, Science **285**, 1036 (2000); I. Chiorescu, Y. Nakamura, C. J. P. M. Harmans, and J. E. Mooij, Science **299**, 1869 (2003).

⁷M. A. Nielsen and I. L. Chuang, *Quantum Computation and Quantum Information* (Cambridge University Press, Cambridge, England, 2000).

⁸S. Han, R. Rouse, and J. E. Lukens, Phys. Rev. Lett. **84**, 1300 (2000).

⁹A. I. Larkin and Yu. N. Ovchinnikov, Phys. Rev. B **28**, 6281 (1983); J. Low Temp. Phys. **63**, 317 (1986).

¹⁰A. I. Larkin and Yu. N. Ovchinnikov, Sov. Phys. JETP **64**, 185 (1986).

¹¹Yu. N. Ovchinnikov and A. Schmid, Phys. Rev. B **50**, 6332 (1994); Yu. N. Ovchinnikov, P. Silvestrini, B. Ruggiero, and A. Barone, J. Supercond. **5**, 481 (1992).

¹²A. I. Larkin and Yu. N. Ovchinnikov, Sov. Phys. JETP **60**, 1060 (1984).

¹³A. I. Larkin and Yu. N. Ovchinnikov, in *Quantum Tunneling in Condensed Media*, edited by Yu. Kagan and A. J. Leggett (Elsevier, New York, 1992).

¹⁴I. S. Gradshteyn and I. M. Ryzhik, *Tables of Integrals, Series, and Products* (Academic Press, San Diego, 1994).

¹⁵L. D. Landau and E. M. Lifshitz, *Quantum Mechanics: Non-relativistic Theory* (Pergamon Press, New York, 1977).

¹⁶R. Migliore and A. Messina, Phys. Rev. B **67**, 134505 (2003).